Int. J. Heat Mass Transfer. Vol. 20, pp. 65–71. Pergamon Press 1977. Printed in Great Britain

THE INFLUENCE OF AXIAL WALL CONDUCTION IN VARIABLE PROPERTY CONVECTION—WITH PARTICULAR REFERENCE TO SUPERCRITICAL PRESSURE FLUIDS

A. WATSON
Simon Engineering Laboratories, University of Manchester, Manchester M13 9PL, England

(*Received* 21 *May* 1976)

Abstract—This paper first analyses the case of flow through a tube, or over a wire, with a heat-transfer coefficient showing a linear dependence on wall temperature, and concludes that axial conduction in the tube wall can combine with the heat-transfer coefficient variation to produce non-uniform steady-state axial temperature distributions. The results of numerical solutions for a more realistic heat-transfer coefficient variation with wall temperature are then presented. The experimental evidence of instability of this type is assessed, the evidence being drawn from supercritical pressure forced and mixed convection experiments.

NOMENCLATURE

B, slope of heat-transfer coefficient decrease;
I, current;
S, dimensionless parameter, $B\Big/\left[\left(\frac{\alpha_0}{q_0}\right)\left(1-\beta\frac{q_0}{\alpha_0}\right)^2\right]$;
T_0, bulk fluid temperature;
T_{0f}, gas side bulk fluid temperature;
T_{pc}, pseudo-critical temperature;
T_w, surface temperature;
X, dimensionless axial coordinate;
Y, dimensionless axial coordinate;
Z, dimensionless temperature;
Z_1, Z_2, roots of equation (11);
b, tube wall thickness;
h, axial step in finite difference calculations;
k, thermal conductivity;
q, heat flux;
q_0, heat flux when $T_w = T_0$;
r, wire radius;
r_i, tube inner radius;
r_0, tube outer radius;
$\bar{r}$, tube mean radius;
t, time;
x, axial coordinate.

Greek symbols

α, heat-transfer coefficient;
α_f, gas side heat-transfer coefficient;
α_0, heat-transfer coefficient when $T_w = T_0$;
β, temperature coefficient of resistance;
ΔT, temperature difference $(T_w - T_0)$;
$\widehat{\Delta T}$, maximum possible temperature difference with gas heating;
κ, thermal diffusivity;
ρ, electrical resistivity;
ρ_0, electrical resistivity at temperature T_0;
θ, dimensionless temperature;
τ, τ', dimensionless time.

1. INTRODUCTION

THERE are a number of problems in which the convective heat-transfer coefficient from a surface depends upon surface temperature, natural convection being an obvious example. Whereas the heat-transfer coefficient increases with increase in surface temperature in natural convection there are some variable property convection flows in which it decreases, for example, heat transfer by forced or mixed convection to supercritical pressure fluids. In these circumstances a surface supplied with heat at a constant rate may be thermally unstable, a slight increase in temperature causing a decrease in convective heat removal and further increase in temperature. This mechanism has been recognised by Stephan [1] and by Kovalev [2], both of whom deduced criteria for avoiding instability. Their concern was the transition and film boiling regimes of pool boiling, in which convective heat removal decreases with increasing temperature difference between surface and fluid and which is thus prone to instability. Their criteria were based upon spacially-independent considerations however. This paper includes the influence of axial conduction along the surface and shows that the instability can lead to stable non-uniform surface temperature distributions. The analysis is applicable to a wire electrically heated by the passage of current and cooled by a crossflow such that the heat transfer coefficient decreases with increasing temperature. This would arise for example in the crossflow of supercritical pressure fluid whose bulk temperature lay below the pseudo-critical temperature T_{pc}, but with the wire temperature above T_{pc}. The analysis is also applied to flow through a tube heated by the passage of current through the tube wall and cooled by convection on the inside, with the same dependence of heat-transfer coefficient on temperature. The case examined first is for linear dependence of heat-transfer coefficient on temperature. Wall temperature distributions for more realistic heat-transfer

coefficient dependence are then presented and the experimental evidence of such distributions is discussed.

2. LINEAR DECREASE OF HEAT-TRANSFER COEFFICIENT WITH INCREASING SURFACE TEMPERATURE

Dealing first with the wire, an energy balance gives

$$\frac{1}{\kappa}\frac{\partial T_w}{\partial t}=\frac{\partial^2 T_w}{\partial x^2}+\frac{I^2\rho}{k(\pi r^2)^2}-\frac{2\alpha\Delta T}{rk}. \tag{1}$$

Radial temperature variations have been neglected and the current is assumed constant. In the absence of axial conduction the heat generated with the wire at temperature T_0 would produce a heat flux.

$$q_0=\frac{I^2\rho_0 r}{2(\pi r^2)^2}.$$

Changing the dependent variable to ΔT, since T_0 is constant,

$$\frac{1}{\kappa}\frac{\partial\Delta T}{\partial t}=\frac{\partial^2\Delta T}{\partial x^2}+q_0\left(\frac{2}{rk}\right)\left(\frac{\rho}{\rho_0}\right)-\left(\frac{2}{rk}\right)\cdot\alpha\Delta T. \tag{2}$$

Introducing dimensionless variables $\tau'=t/(r^2/\kappa)$, $X=x/r$ and $\theta=\Delta T/(q_0/\alpha_0)$ where α_0 is the heat-transfer coefficient when ΔT is zero, equation (2) can be re-written

$$\frac{\partial\theta}{\partial\tau'}=\frac{\partial^2\theta}{\partial X^2}+\left(\frac{2r\alpha_0}{k}\right)\left[\left(\frac{\rho}{\rho_0}\right)-\left(\frac{\alpha}{\alpha_0}\right)\cdot\theta\right]. \tag{3}$$

We can now introduce resistivity and heat-transfer coefficient variations

$$\left.\begin{aligned}\rho&=\rho_0(1+\beta\Delta T)\\ \alpha&=\alpha_0(1-B\Delta T)\end{aligned}\right\} \tag{4}$$

and

to give

$$\frac{\partial\theta}{\partial\tau'}=\frac{\partial^2\theta}{\partial X^2}+\left(\frac{2r\alpha_0}{k}\right)\left\{1-\left(1-\frac{\beta q_0}{\alpha_0}\right)\theta+\frac{Bq_0}{\alpha_0}\cdot\theta^2\right\}. \tag{5}$$

With further substitutions,

$$\left.\begin{aligned}&Z=\left(1-\frac{\beta q_0}{\alpha_0}\right)\cdot\theta,\quad Y=\left[\left(1-\frac{\beta q_0}{\alpha_0}\right)\left(\frac{2r\alpha_0}{k}\right)\right]^{1/2}\cdot X\\ &\text{and}\\ &\tau=\left(\frac{2r\alpha_0}{k}\right)\left(1-\frac{\beta q_0}{\alpha_0}\right)\cdot\tau'.\end{aligned}\right\} \tag{6}$$

we get a single parameter equation,

$$\frac{\partial Z}{\partial\tau}=\frac{\partial^2 Z}{\partial Y^2}-Z+S\cdot Z^2+1 \tag{7}$$

where

$$S=\frac{B}{\left(\frac{\alpha_0}{q_0}\right)\left(1-\frac{\beta q_0}{\alpha_0}\right)^2}.$$

The same approach may be adopted for the analysis of the tube. Assuming the tube wall to be thin so far as radial temperature variations are concerned, and to be insulated on its outer surface, the energy balance is:

$$\frac{1}{\kappa}\frac{\partial T_w}{\partial t}=\frac{\partial^2 T_w}{\partial x^2}+\frac{I^2\rho}{(2\pi\bar{r}b)^2k}-\alpha(T_w-T_0)\left(\frac{r_i}{\bar{r}bk}\right). \tag{8}$$

Neglecting the variation of bulk temperature with x and t allows the dependent variable to be changed to ΔT. This is exact for two phase equilibrium flows in which T_0 is the saturation temperature. It is a good approximation for supercritical pressure fluids in the region of $T_0=T_{pc}$. Introducing dimensionless variables $\tau'_T=t/(\bar{r}^2/\kappa)$, $X_T=x/\bar{r}$ and θ as before gives the equivalent of equation (3)

$$\frac{\partial\theta}{\partial\tau'_T}=\frac{\partial^2\theta}{\partial X_T^2}+\left(\frac{\alpha_0 r_i\bar{r}}{bk}\right)\left\{\left(\frac{\rho}{\rho_0}\right)-\left(\frac{\alpha}{\alpha_0}\right)\cdot\theta\right\}. \tag{9}$$

Only the dimensionless parameter incorporating thermal conductivity differs between equations (3) and (9), the difference arising from geometry, and substitutions from equation (4) lead to an equation identical to equation (7). The thermal conduction parameter changes the form of Y and τ which become

$$Y_T=\left[\left(1-\frac{\beta q_0}{\alpha_0}\right)\left(\frac{\alpha_0 r_i\bar{r}}{bk}\right)\right]^{1/2}\cdot X,$$

$$\tau_T=\left(\frac{\alpha_0 r_i\bar{r}}{bk}\right)\left(1-\frac{\beta q_0}{\alpha_0}\right)\cdot\tau'_T.$$

The suffix T referring to the tube will be omitted from now on, since the solutions of equation (7) will be presented in dimensionless variables.

(a) *Steady state solutions*

In the steady state, equation (1) becomes

$$0=\frac{\mathrm{d}^2 T_w}{\mathrm{d}x^2}+\frac{I^2\rho}{k(\pi r^2)^2}-\frac{2\alpha\Delta T}{rk} \tag{10}$$

from which it is clear that axial conduction makes up the difference between heat generated and heat removed. This difference is shown by Fig. 1(a) in which convective heat removal for some arbitrary value of B is plotted against ΔT. Heat generated is also shown (full lines, the curves shown dotted will be discussed later). At two values of ΔT a balance occurs. In terms of dimensionless temperature the two values of ΔT represent the roots of the equation [from equation (7)].

$$SZ^2-Z+1=0. \tag{11}$$

For $0<S<\frac{1}{4}$ there are two real roots. That corresponding to ΔT_1 in Fig. 1 is a stable solution—an increase in ΔT away from this value improves convective heat removal and provides a restoring action. The root corresponding to ΔT_2 in Fig. 1 is unstable. For $S=\frac{1}{4}$ there is a single real root, the significance being apparent from Fig. 1(b). $S=0$ is the case of constant heat-transfer coefficient. The loci of the roots of equation (11) are plotted in Fig. 2. Solutions of equation (7) in its steady state form have been carried out for the case of a semi-infinite wire or tube, specifying Z and $(\partial Z/\partial Y)$ (temperature level and temperature gradient) at the finite end. The variations of Z with Y are shown in Fig. 3, and it can be seen that with an adiabatic end at a prescribed temperature level lying within the envelope of Fig. 2, spacial variations of temperature occur. In terms of Fig. 1 these represent oscillations of temperature about ΔT_2; the

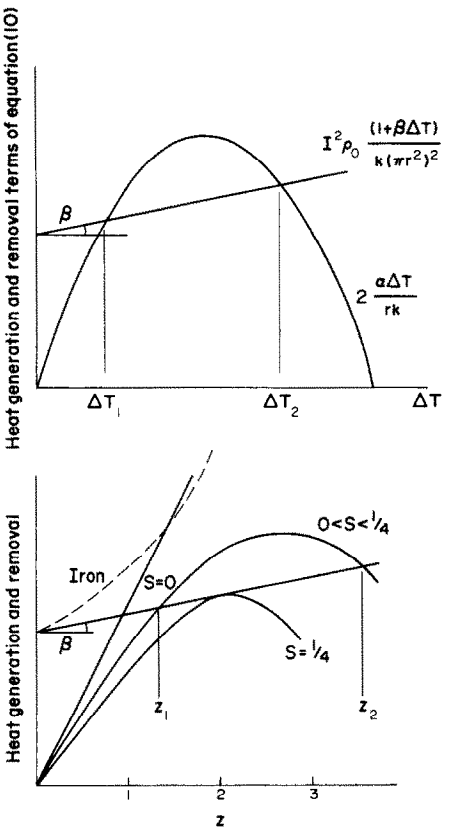

FIG. 1. Heat generation and convective removal vs real and dimensionless temperature differences.

amplitude of a typical oscillation is shown in Fig. 2. Initial prescribed temperatures lying outside the envelope produce variations of Z with no limit and indicate that no steady state is possible under these circumstances. Varying the initial slope does influence the solutions and very high initial slopes can produce unrealistic values of Z, indicating no steady state, even for initial values of Z within the envelope of Fig. 2.

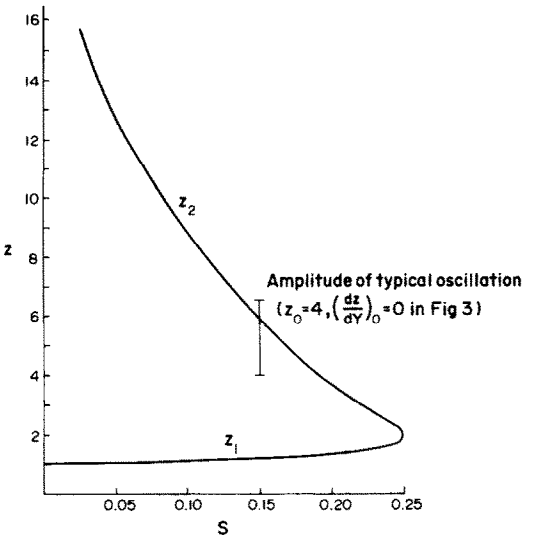

FIG. 2. Loci of roots of equation (11).

A variety of solutions is shown in Fig. 3 for $S = 0.15$. In terms of actual distance x, the wavelength of the temperature variation is governed by the group $(2r\alpha_0/k)$ for the wire and $(\alpha_0 r_i \bar{r}/bk)$ for the tube. These represent the ratio of thermal resistances of convection and of axial conduction. Thus the temperature distributions "necessary" to make up the balance between heat supply and removal depend upon the geometry and material of the tube or wire.

Although the temperature variation of resistivity has been taken as linear in the analysis, some metals, e.g. iron, have a quadratic variation. Fig. 1(b) shows that in this case even for constant heat-transfer coefficient, two intersections are possible and stable non-uniform temperature distributions could in principle occur.

(b) *Transient solutions*

The final steady state solutions discussed above may not occur in general, and solutions of the transient equations have been carried out for a finite length of

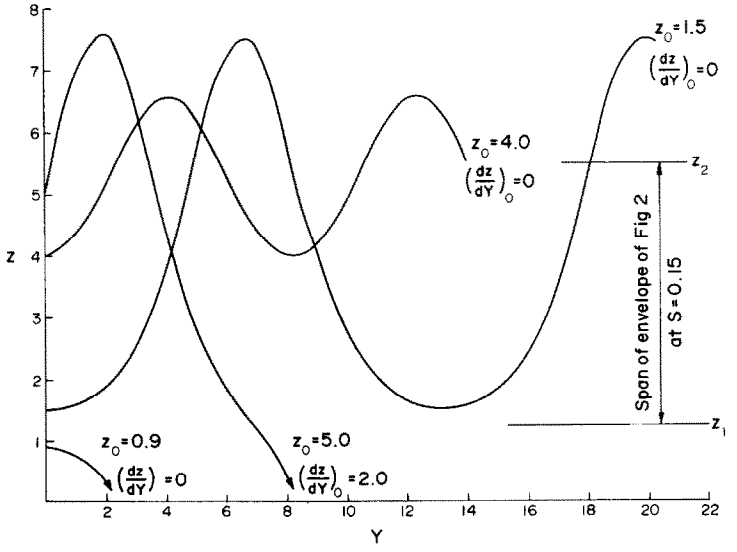

FIG. 3. Steady state dimensionless temperature distributions for $S = 0.15$ and various boundary conditions.

the tube considered to be made up of typically 80 elements each of length h ($h = r_i/2$ was used). The set of finite difference equations

$$\frac{(Z_{i+1}+Z_{i-1}-2Z_i)}{h^2} - Z_i + SZ_i^2 + 1 = \frac{dZ_i}{d\tau} \quad (12)$$

were solved using the Runge–Kutta method. The form of the Z solution depends upon how much of the envelope of Fig. 2 is spanned by the initial temperature distribution. Figure 4(a) shows the solutions for a linear temperature distribution at time $\tau = 0$ with the ends held isothermal, one end lying within the envelope and the other outside at a higher Z. With the entire distribution lying within the envelope, or with one end

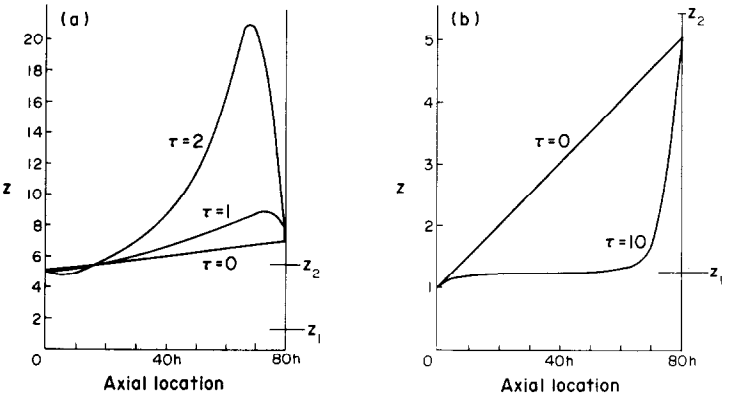

FIG. 4. Transient dimensionless temperature distributions for different initial conditions.

below, Fig. 4(b), the stable solution $Z = Z_1$ occurs over a long length of the tube. Figure 4(a) does not reach a steady state because of the linear α variation, which gives negative heat-transfer coefficients at high ΔT values.

3. SOLUTIONS FOR MORE REALISTIC HEAT-TRANSFER COEFFICIENTS

A change in the character of Fig. 1 occurs for heat-transfer coefficients which decrease with increasing ΔT but reach a minimum positive value, Fig. 5. The α distribution is shown inset and is typical of pure forced

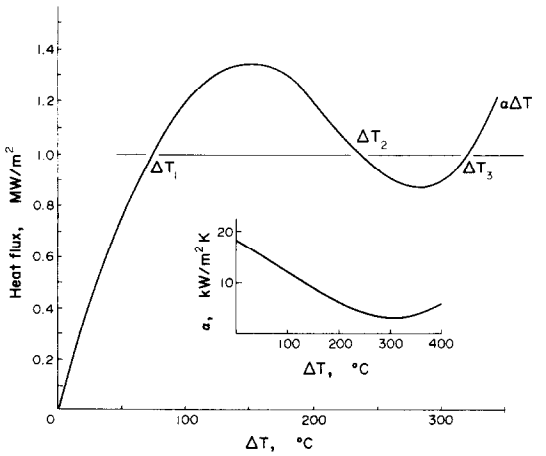

FIG. 5. Heat-transfer coefficient and convective heat removal vs temperature difference for typical supercritical pressure forced convection experiments.

convection to supercritical pressure fluids in the absence of buoyancy effects when bulk temperature lies below T_{pc} and wall temperature lies above T_{pc}. The actual values used here correspond to the experiments of Harrison [6] who measured wall temperature distributions for supercritical pressure water at 245 bars flowing under forced convection through small bore stainless steel tubes. There is disagreement between the values of α predicted by the correlations for supercritical pressure fluids [9], although all show the same trend, hence the choice of this particular data. There are now, in Fig. 5, three intersections of the heat generation and removal curves, the centre one being unstable. Oscillations of temperature about ΔT_2 can occur but lie within limiting values corresponding to ΔT_1 and ΔT_3.

(a) *Steady state solutions*

Figure 6 shows solutions of equation (8) in steady state form, using the data of Fig. 5. The end condition for the semi-infinite tube or wire is adiabatic at various temperature levels. Constant heat supply rate has been assumed for simplicity, $\beta = 0$. Figure 5 shows that oscillations may take place for heat fluxes of about $0.87 < q_0 < 1.35\,\text{MW/m}^2$. Initial temperature levels between ΔT_1 and ΔT_2 produce oscillations rising to a maximum between ΔT_2 and ΔT_3, whilst initial temperature levels between ΔT_2 and ΔT_3 show a decrease in temperature. Too low an initial value of ΔT, e.g. 100°C, causes unrealistic temperatures above ΔT_3 to be reached, indicating no permissible steady state solution. Initial values very close to ΔT_3 produce a very flat topped variation.

(b) *Transient solutions*

Transient solutions of equation (8) have been obtained exactly as in Section 2(b), with the heat transfer data of Figs. 5 and 6. A sample of results is shown in Fig. 7, which represents the temperature distributions along a section of tube with isothermal ends held at $\Delta T = 200$°C. The three solutions are for various initial temperature levels, the distribution being uniform in each case. If the initial distribution is close enough to the stable value ΔT_1 or ΔT_3, the final distribution is

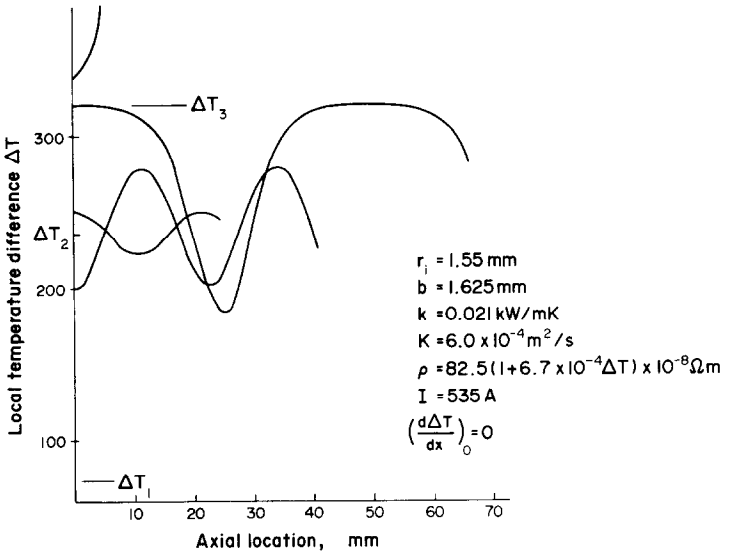

FIG. 6. Steady state wall temperature distributions for the data of Fig. 5 with a particular small bore tube and various initial temperature levels.

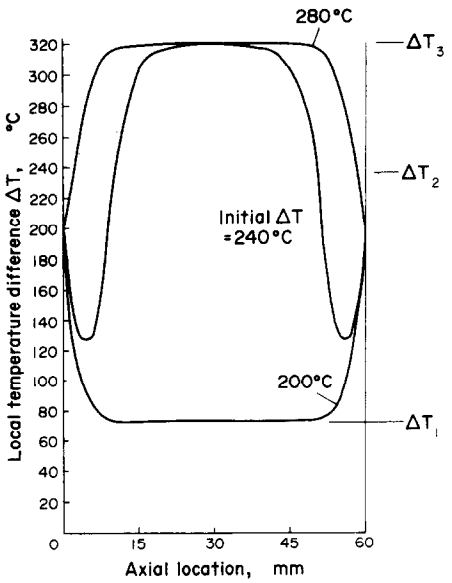

FIG. 7. Wall temperature distributions after time $t = 10$ s for a tube with isothermal ends and various uniform initial levels of ΔT.

simple. A more complicated distribution with oscillations about ΔT_2 is shown. Changes in the distributions after time $t = 10$ s were negligible.

4. EXPERIMENTAL EVIDENCE

The evidence is all from supercritical pressure heat-transfer experiments, which are perhaps unique in the variety of well defined irregularities of wall temperature distribution which have been measured. The heat-transfer coefficient is known to vary with mass flow rate, pressure, and wall and bulk temperatures in forced convection flows under these conditions, and although the variation of bulk temperature along a tube is frequently small when near T_{pc}, it is probable that the heat removal curve such as Fig. 5 would vary with axial location. This would distort the temperature distributions from the idealised ones calculated above. As a result of such considerations the experimental evidence is not as clear as one would prefer. There are three types of irregularity of wall temperature distribution which form the main evidence.

(a) *Buoyancy peaks*

Sharp peaks in wall temperature have been observed in forced flows in tubes with the flow vertically upwards; under identical conditions with the flow vertically downwards they do not occur. Hall and Jackson [3] formulated a model to explain the effect based upon the idea that buoyancy forces acting upwards with the forced flow reduced the level of shear stress and hence the turbulence production rate. When this occurred near the wall in the region of maximum turbulence production the heat-transfer coefficient was reduced. The buoyancy forces are wall temperature dependent and in terms of the present model they present a mechanism by which heat-transfer coefficient may decrease with increasing wall temperature. In several experiments (e.g. Jackson and Evans-Lutterodt [4] double peaks have been observed, Fig. 8. These peaks are quite narrow in axial extent. In terms of the present model the sharpness and wavelength is interpreted as being due to the thermal instability and the conductive properties of the tube, rather than to a reduction and subsequent recovery of turbulence production. Thus multiple peaks will occur if the axial extent of the flow having a convective heat removal curve as in Fig. 5 is long compared with the corresponding temperature wavelength. The experimental evidence of Hall and Jackson [3] shows some evidence of reductions in wall temperature immediately upstream of a peak, similar to Fig. 7.

(b) *Localised reductions in wall temperature*

Figure 9 shows some data of Domin [5] which appear to correspond in type to those of Fig. 6 with

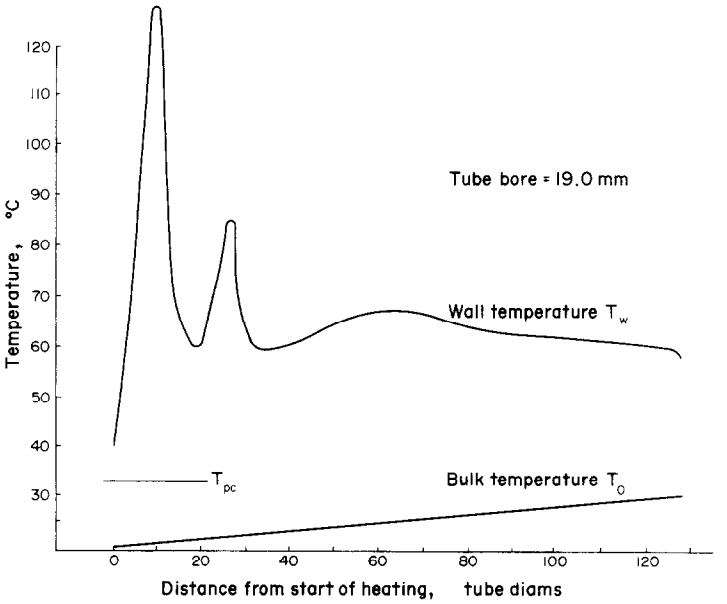

FIG. 8. Data of [4], for mixed convection to supercritical pressure CO_2 at 74.5 bar.

initial temperatures close to ΔT_3. The wall temperatures upstream of the reduction are much higher than T_{pc} ($T_{pc} \approx 386°C$ under these conditions) so that the level of heat-transfer coefficient would be relatively low and the ΔT values high in terms of Fig. 5.

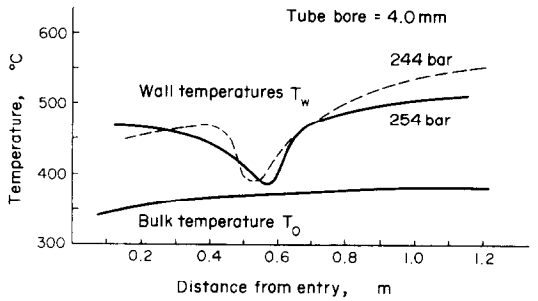

FIG. 9. Data of [5] for forced convection to supercritical pressure water.

(c) *Multiple peaks in buoyancy free flows*

Figure 10 shows the data of Harrison [6]. The peaks built up slowly from the downstream end of the tube towards the location at which $T_w = T_{pc}$, which remained steady throughout. It is for $T_w > T_{pc}$ that α begins to deteriorate with increasing T_w. Harrison's experiments were carried out with the test section horizontal so the deterioration in α is due to property variations and not buoyancy effects. The assumption of $T_0 =$ constant is relatively good in these experiments and the heat removal curve of Fig. 5 is less likely to change radically with x. In upwards buoyancy influenced flows the natural convection improves the heat-transfer coefficient after only a relatively short axial extent, which may account for no more than two peaks occurring in these cases. Although the temperature distributions

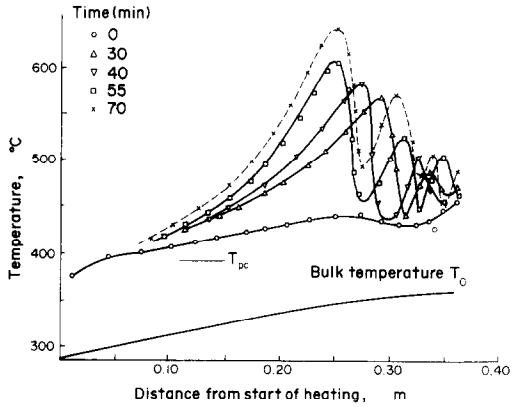

FIG. 10. Transient wall temperature measurements from [6] for forced convection to supercritical pressure water in a 3.1 mm bore tube.

of Fig. 10 compare with the semi-infinite steady-state tube distributions of Figs. 3 and 6, it is not clear why growth took place from the downstream end of the tube. Ormatsky, Glushenko, Siomin and Kalatcher [7] have reported similar multi-peaked distributions in experiments of supercritical pressure water flowing through bundles of heated rods.

5. DISCUSSION

The experimental data selected as evidence of the proposed mechanism represents the extremes of wall temperature variation. Indeed, it is only the extreme nature of these sets of results which allows the mechanism to be identified; with less significant wall temperature variations the α distribution and its axial variation are not known precisely enough in supercritical pressure flows to allow a high degree of agreement between prediction and experiment to be obtained. In terms of Fig. 5 severe wall temperature

variations are caused by a large difference between ΔT_1 and ΔT_3. Heat-transfer coefficients less sensitive to wall temperature would cause the maximum and minimum in $\alpha\Delta T$ to be more nearly equal, resulting in smaller wall temperature variations.

The literature on supercritical pressure fluids contains many correlations (see for example the review by Hall, Jackson and Watson [9]) which should, but do not, agree with one another. Part of the difficulty in obtaining agreement between data produced by different workers under apparently similar conditions may be due to neglect of the effects considered here.

6. CONCLUSIONS

(a) For a semi-infinite tube or wire heated electrically and cooled by convection such that the heat-transfer coefficient decreases with increase in temperature it has been shown that non-uniform steady-state axial temperature distributions can occur.

(b) Transient numerical calculations for tubes of finite length have shown that similar non-uniform temperature distributions may occur, depending upon the initial conditions.

(c) The evidence of this type of phenomenon having occurred in supercritical pressure flows has been examined. Three different types of measured wall temperature distribution with extreme variations correspond in shape to those calculated.

Acknowledgements—The author is indebted to a referee and to his colleagues, especially Dr. P. H. Price and Mr. C. Tye, for valuable advice.

REFERENCES

1. K. Stephen, Stabilität beim Sieden, *Brennst.-Wärme-Kraft* **17**(12), 571–614 (1965).
2. S. A. Kovalev, On methods of studying heat transfer in transition boiling, *Int. J. Heat Mass Transfer* **11**, 279 (1968).
3. W. B. Hall and J. D. Jackson, Laminarisation of a turbulent pipe flow by buoyancy forces, ASME Paper 69-HT-55 (1969).
4. J. D. Jackson and K. Evans-Lutterodt, Impairment of turbulent forced convection heat transfer to supercritical pressure CO_2 caused by buoyancy forces, Internal Report NE2, Simon Eng. Labs., University of Manchester 1968.
5. G. Domin, Wärmeübergang in Kritischen under überkritischen Bereichen von Wasser in Rohren, Brennst.-Wärme-Kraft **15**(11), 527–532 (1963).
6. G. S. Harrison, Heat transfer to supercritical pressure water flowing in small bore tubes, Ph.D. Thesis, University of Manchester (1973).
7. A. P. Ormatsky, L. F. Glushenko, E. T. Siomin and S. I. Kalatcher, The research of temperature conditions of small diameter parallel tubes cooled by water under supercritical pressures, Paper B.8.11, 4th International Heat Transfer Conference, Versaille (1970).
8. M. E. Shitsman, Impairment of heat transmission at supercritical pressures, *Teplofiz. Vysok. Temper.* **1**(2), 237–244 (1963).
9. W. B. Hall, J. D. Jackson and A. Watson, A review of forced convection heat transfer to fluids at supercritical pressures, *Proc. Instn Mech. Engrs* **182**, Part 3I, (1968).

INFLUENCE DE LA CONDUCTION LONGITUDINALE EN PAROI SUR LA CONVECTION A PROPRIETES VARIABLES, AVEC REFERENCE PARTICULIERE AUX FLUIDES A PRESSION SUPERCRITIQUE

Résumé—L'article analyse tout d'abord le cas d'un écoulement dans un tube ou autour d'un fil, avec un coefficient de convection dépendant linéairement de la température de la paroi et il conclut que la conduction longitudinale dans la paroi du tube se compose avec la variation du coefficient de convection pour produire une distribution longitudinale et permanente de température. On présente ensuite les résultats numériques pour une variation plus réelle du coefficient de convection en fonction de la température pariétale. On dégage une instabilité accessible expérimentalement, surtout dans le cas de la convection forcée ou mixte aux pressions supercritiques.

DER EINFLUSS DER AXIALEN WANDWÄRMELEITUNG BEI STRÖMUNGEN MIT VERÄNDERLICHEN STOFFEIGENSCHAFTEN—UNTER BESONDERER BERÜCKSICHTIGUNG VON FLUIDEN BEI ÜBERKRITISCHEN DRÜCKEN

Zusammenfassung—In dieser Arbeit wird zunächst der Fall einer Strömung durch ein Rohr bzw. über einen Draht untersucht, wobei der Wärmeübergangskoeffizient linear von der Wandtemperatur abhängt; hieraus wird gefolgert, daß eine axiale Wärmeleitung in der Rohrwand zusammen mit der Variation des Wärmeübergangskoeffizienten nichtgleichförmige, stationäre, axiale Temperaturverteilungen hervorrufen kann. Anschließend werden numerisch ermittelte Ergebnisse für realistischere Veränderungen des Wärmeübergangskoeffizienten mit der Wandtemperatur vorgestellt. Unter Verwendung von Experimenten bei erzwungener und gemischter Konvektion bei überkritischen Drücken wird eine Instabilität dieser Art nachgewiesen.

ВЛИЯНИЕ ТЕПЛОПРОВОДНОСТИ СТЕНКИ В ОСЕВОМ НАПРАВЛЕНИИ В СЛУЧАЕ КОНВЕКЦИИ С УЧЕТОМ ИЗМЕНЕНИЯ СВОЙСТ ЖИДКОСТЕЙ ПРИ СВЕРХКРИТИЧЕСКОМ ДАВЛЕНИИ

Аннотация — Рассматривается течение в трубе или вдоль проволочки, когда коэффициент теплообмена линейно зависит от температуры стенки. Делается вывод о том, что теплопроводность стенки трубы в осевом направлении совместно с изменением коэффициента теплообмена может вызвать неоднородные стационарные распределения температуры вдоль оси. Приводятся численные результаты для случая изменения коэффициента теплообмена в зависимости от температуры стенки. Такое распределение для случая вынужденной и смешанной конвекции при сверхкритическом давлении подтверждается экспериментами.